NATIONAL ADVISORY COMMITTEE FOR AERONAUTICS

TECHNICAL NOTE 3056

A FLIGHT INVESTIGATION OF LAMINAR AND TURBULENT BOUNDARY LAYERS PASSING THROUGH SHOCK WAVES AT FULL-SCALE REYNOLDS NUMBERS

By Eziaslav N. Harrin

Langley Aeronautical Laboratory
Langley Field, Va.

NACA

Washington

December 1953

NATIONAL ADVISORY COMMITTEE FOR AERONAUTICS

————

TECHNICAL NOTE 3056

————

A FLIGHT INVESTIGATION OF LAMINAR AND TURBULENT

BOUNDARY LAYERS PASSING THROUGH SHOCK WAVES

AT FULL-SCALE REYNOLDS NUMBERS

By Eziaslav N. Harrin

SUMMARY

An investigation has been made in flight at free-stream Mach numbers up to 0.76 to determine the behavior of laminar and turbulent boundary layers passing through shock waves at Reynolds numbers up to 26×10^6. The free-stream Mach numbers obtained in the tests were sufficiently high to give extensive regions of local supersonic flow. Boundary-layer and pressure-distribution measurements were made on a short-span airfoil built around a wing of a fighter airplane. Laminar flow up to the position of the shock wave was obtained on the upper surface of the smooth airfoil. Turbulent flow ahead (upstream) of the shock wave was obtained by attaching a transition strip near the nose.

The results of the investigation indicated that the abrupt increase in momentum thickness and displacement thickness in the region of the pressure rise associated with a shock wave was significantly less with laminar than with turbulent flow ahead of the shock wave. With laminar flow ahead of the shock wave, transition from laminar to turbulent flow was caused by the abrupt pressure rise of the shock wave and was accompanied by a large decrease in the value of the boundary-layer shape parameter H through the shock wave. The beneficial effect of having laminar flow ahead of the shock wave was indicated by 50-percent smaller values of momentum thickness and lower values of shape parameter (1.6 as compared with 2.9) downstream of the shock waves.

Comparison of the present results with results obtained at low Reynolds numbers by other investigators indicated that with turbulent flow ahead of the shock wave the changes in boundary-layer characteristics through the shock wave were not much different for the full-scale than for the 1/10-scale data. With laminar flow ahead of the shock wave, the changes in momentum thickness and displacement thickness (expressed as a fraction of a characteristic length) were about 10 times as great for the 1/23-scale as for the full-scale data.

INTRODUCTION

Information obtained at low chord Reynolds numbers (up to 2.6×10^6 or 1/10 full scale) has indicated large differences between airfoil pressure distributions with laminar boundary-layer flow and those with turbulent boundary-layer flow ahead (upstream) of shock waves. These differences are of such magnitude as to cause serious force and moment differences and, further, indicate large differences in the characteristics of boundary layers passing through shock waves (see, for example, ref. 1).

Since these phenomena have a direct bearing on present and future airplane design, a flight investigation was undertaken to extend the information to full-scale chord Reynolds numbers. Partial results of this investigation, reported in reference 2, indicated minor differences in airfoil pressure distributions with laminar and with turbulent flow ahead of shock waves. The second and final phase of the flight investigation at full-scale Reynolds numbers, reported herein, was concerned with the changes in laminar and turbulent boundary layers passing through shock waves.

The full-scale tests included measurements of the chordwise pressure distribution and boundary-layer characteristics at chord Reynolds numbers from 17×10^6 to 26×10^6. The measurements were made in dives up to a free-stream Mach number of about 0.76, which was sufficiently high to give extensive regions of supersonic flow about the test area.

SYMBOLS

C_L airplane lift coefficient

c airfoil chord

H boundary-layer shape parameter, δ^*/θ

l length of supersonic region with turbulent flow in boundary layer

M Mach number

P pressure coefficient, $\dfrac{p_\delta - p_0}{q_0}$

p static pressure

p_T total pressure

q_o free-stream dynamic pressure, $\frac{1}{2}\rho_o V_o^2$

R_c Reynolds number based on free-stream conditions and chord of airfoil, $V_o\rho_o c/\mu_o$

R_l Reynolds number based on free-stream conditions and length of turbulent supersonic region l

R_θ boundary-layer Reynolds number based on local condition immediately outside boundary layer and on momentum thickness, $u_\delta\rho_\delta\theta/\mu_\delta$

u velocity in boundary layer in x-direction

V_o free-stream velocity

x chordwise distance from leading edge along surface of test airfoil or curved plate

y distance perpendicular to surface of test airfoil

δ outer edge of boundary layer

δ^* displacement thickness, $\displaystyle\int_0^\delta \left(1 - \frac{\rho u}{\rho_\delta u_\delta}\right)dy$

θ momentum thickness, $\displaystyle\int_0^\delta \frac{\rho u}{\rho_\delta u_\delta}\left(1 - \frac{u}{u_\delta}\right)dy$

μ coefficient of viscosity

ρ mass density

Subscripts:

δ outer edge of boundary layer

o free stream

APPARATUS AND TESTS

Boundary-layer and pressure-distribution measurements were made on an airfoil built around the wing of a fighter airplane (fig. 1). This test airfoil had a chord of 89.0 inches, a span of 60 inches, and a

maximum thickness of 16 percent chord. The airfoil section was approximately an NACA 64-series section. The test airfoil was constructed of laminated wood and was covered with a 1/8-inch-thick sheet of aluminum to provide a smooth and stable surface. Actually, two airfoils were built and one was mounted on each wing. Only the left airfoil was used for the measurements; the right was used to provide lateral balance to the airplane.

Static-pressure orifices were installed on the upper surface at 0.35 chord and every 0.025 chord from 0.425 to 0.65 chord (see fig. 2). In some preliminary tests, circular orifices 1/16 inch in diameter were used. However, flow in or out of the orifices, resulting from variations of pressure at the orifices associated with varying speed and altitude, caused premature transition. A special shape of orifice was therefore designed in an effort to minimize this adverse effect on the laminar boundary layer. This orifice consisted of a slit 0.6 inch long (spanwise) and 0.003 inch wide (chordwise) which opened into a small plenum chamber and tubing that led to the pressure recorder. Spreading the flow spanwise through the orifice successfully reduced the point disturbance to the laminar boundary layer and thereby prevented premature transition to turbulent flow.

Total-pressure measurements through the boundary layer were made with boundary-layer rakes consisting of 8 to 10 total-pressure probes. Shown in figure 2 are two rakes, each with 8 probes, half of which are obscured in the photograph by the presence of the others. These probes were made from stainless-steel tubing of 0.06-inch inside diameter and 0.015-inch wall thickness or from brass tubing of 0.06-inch inside diameter and 0.03-inch wall thickness. The upstream end of each tube was flattened and filed into a rectangular opening 0.003 inch high and 0.1 inch long with a wall thickness of about 0.003 inch.

The boundary-layer rakes were used either singly and set 4 inches inboard of the orifices, or in pairs and set about 1 inch on each side of the line of orifices. All laminar-flow measurements were made with only one rake on the test surface, except for the 0.55- and 0.575-chord stations. In this case, the 0.575-chord rake was located approximately

2 inches outboard and $2\frac{1}{4}$ inches downstream of the rake at 0.55 chord. The heights of the tubes above the surface were measured before and after each flight. In most cases there was no difference in tube heights before and after flight. Where changes had occurred, the maximum was of the order of 0.005 inch.

In evaluating the velocity and density distributions in the boundary layer, the static pressure and total temperature through the boundary layer were assumed to be constant.

All the measurements were made in dives, which were started by "pushing over" at an altitude of 28,000 feet and a Mach number of 0.60 to a dive angle of 38° and which were continued until an airplane Mach number of 0.76 was reached; then a gradual pull-out was begun. Data were recorded from a Mach number of 0.60 up to the highest Mach number attained, which was approximately 0.77. Lift coefficients during the portion of the dives in which the measurements were made varied from approximately 0.16 to 0.08 at the high-speed end of the dive. The range of free-stream Reynolds number (based on the chord of the test airfoil section) for these tests was from 17×10^6 to 26×10^6.

Boundary-layer and static-pressure measurements were made with the smooth-surfaced test airfoil and with a transition strip consisting of a thread of 0.036-inch diameter taped to the upper surface at 0.04 chord.

Free-stream total pressure p_{T_0} and static pressure were measured by means of a pitot-static tube mounted on a boom about 1 chord ahead of the airplane wing tip. The measured static pressures were corrected to free-stream static pressures p_0.

Pressures were measured with low-lag NACA recording multiple manometers. Normal acceleration used for determining the airplane lift coefficient was measured by using an NACA air-damped recording accelerometer.

RESULTS

The distributions of Mach number through the boundary layer at several chordwise stations on the upper surface are presented for three values of free-stream Mach number in figures 3 and 4 with laminar and turbulent boundary layers, respectively, ahead of the shock waves. The laminar boundary layer was obtained with the smooth airfoil and the turbulent boundary layer with a transition strip at 0.04 chord on the upper surface. The boundary-layer profiles at the various chordwise stations were selected at as nearly the same nominal values of free-stream Mach number, airplane lift coefficient, and Reynolds number as was possible with the available data. The limits within which it was possible to select the data conditions are indicated in the sublegends of figures 3 and 4; the actual free-stream Mach numbers and airplane lift coefficients are indicated in the tables adjacent to each group of boundary-layer profiles.

For a number of the profiles the results of two test runs were used, particularly at chordwise stations where the boundary-layer profiles were changing rapidly. At such chordwise stations some differences between results of the two test runs may be seen in the boundary-layer profiles.

    The shapes of the profiles near the surface were probably unaffected
by the size of the total-pressure tube used in the rake. According to
criteria established in reference 3, such effects would be negligible for
the conditions encountered in these tests. The effects of the rake on
the flow conditions, however, are not known. The shape of the profile
near the surface may be affected to some extent by lag in the pressure
measurements.

    The boundary-layer profiles in figures 3 and 4 were evaluated to give
a chordwise distribution of momentum thickness θ, displacement thickness
δ^*, shape parameter H, and boundary-layer Reynolds number R_θ, as shown
in figure 5 with laminar flow ahead of the shock wave and in figure 6
with turbulent flow ahead of the shock wave. Included in figures 5 and 6
are chordwise distributions of the static-pressure coefficient P, aver-
aged for indicated flight conditions of free-stream Mach number and air-
plane lift coefficient. The maximum local Mach number and the local Mach
number of 1.0 are indicated on the pressure distributions.

    A comparison has been made, on a somewhat indirect basis, between
the present results obtained at high Reynolds numbers and the results of
reference 1 obtained at low Reynolds numbers. A conventional comparison
on the basis of wing chord as the reference length and free-stream Mach
number as the common condition was not possible, inasmuch as the results
of reference 1 were obtained on a curved plate in a curved channel and
the effective free-stream Mach number was not given. With turbulent flow
ahead of the shock wave and with the same maximum local Mach number, the
pressure distribution in the supersonic region on the plate was, fortui-
tously, very similar to that in the supersonic region on the wing. At a
free-stream Mach number of 0.752 for the flight tests, the same maximum
local Mach number (1.32) was obtained as in the channel tests. For this
condition the supersonic region extended from 72.2 millimeters to
218.8 millimeters on the plate and from 0.205 to 0.59 chord on the wing.
The correspondence of the pressure distributions for the turbulent-flow
case was considered as establishing that the surface contours or boundary
conditions in the designated regions were effectively similar for the
flight and channel tests and that the length of the supersonic regions
could be used as the reference length in comparing the boundary-layer
characteristics in the region of the shock waves for the turbulent-flow
case to indicate the effect of Reynolds number. Since the measurements
with laminar flow ahead of the shock waves were obtained in both investi-
gations for the same effective free-stream Mach number as with turbulent
flow, the length of the supersonic regions obtained with turbulent flow
could also be used as the reference length for comparing the pressure
distributions and the boundary-layer characteristics with laminar flow
ahead of the shock waves to indicate the effect of Reynolds number for
this case. A further justification for the use of this characteristic
length is that the values of boundary-layer thicknesses $(\theta/l$ and $\delta^*/l)$

ahead of the shock wave for high and low Reynolds numbers were found to compare well when adjustment was made for the difference in the Reynolds numbers (based on the characteristic length l). This adjustment can be made by assuming that the dimensionless boundary-layer thicknesses vary inversely as the square root of the Reynolds number R_l for the laminar layer, and inversely as the fifth root for the turbulent layer.

Comparison of the results at high and low Reynolds numbers is made in figure 7 for a laminar boundary layer ahead of the shock wave and in figure 8 for a turbulent boundary layer ahead of the shock wave. The data for the flight tests in figures 7 and 8 have not been previously presented in this paper. The values of R_θ indicated in figures 7 and 8 are for local conditions immediately ahead of the first shock wave for the data of reference 1 and at minimum pressure for the present data. The pressure distributions ahead of $x/l = 0.335$ for the flight results were obtained from other tests in which such information was available. The pressure distributions ahead of $x/l = 0.46$ for the turbulent flow conditions of reference 1 were obtained by interpolation of the data presented in that reference.

DISCUSSION

Laminar Flow Ahead of the Shock Wave

At a free-stream Mach number of 0.710 the difference between the boundary-layer profiles at the 0.45- and 0.50-chord stations (fig. 3(a)) indicates that transition from laminar to turbulent flow begins in the region of the pressure rise associated with the shock wave between 0.45 and 0.50 chord. (That the flow ahead of the shock wave was laminar may be judged by the boundary-layer thickness, by the shape of the boundary-layer Mach number profiles, by the high value of shape parameter compared with that of an unseparated turbulent boundary layer, and by the fact that separation of a turbulent boundary layer necessary to give this high value of shape parameter would not be expected in the favorable pressure gradient ahead of the shock wave.) The chordwise variation of displacement thickness and momentum thickness was gradual (fig. 5(a)). Through the shock wave, the shape parameter H decreased from a value of about 3.2 to a value of 1.8 as transition to turbulent flow occurred. Local separation was not evident at the stations where the measurements were made. The boundary-layer Reynolds number R_θ had a value of 2,800 ahead of the shock wave and the maximum local Mach number M_δ was 1.16.

At a free-stream Mach number of 0.736, laminar separation appears to have occurred at about 0.50 chord, with subsequent transition to

turbulent flow and reattachment being completed at about 0.60 chord
(fig. 3(b)). The chordwise variation of displacement thickness and
momentum thickness (fig. 5(b)) indicated sudden increases in the values
of these parameters through the region of the pressure rise associated
with the shock wave.

The shape parameter H increased slightly in the region of decreas-
ing pressures just upstream of the shock wave and had values of about
3.6. Such high values of shape parameter are usually associated with
imminent separation or separation. For the Reynolds numbers of the
present tests, the results of reference 4 indicate that separation of
the laminar boundary layer could be caused by a pressure increase corre-
sponding to a pressure coefficient of the order of 0.01, a value well
within the accuracy of the measurements in the present tests. In the
region of abrupt pressure rise associated with the shock wave, the shape
parameter H decreased abruptly from a value of 3.6 to 1.8, indicating
completion of transition to turbulent flow. The boundary-layer Reynolds
number immediately ahead of the shock wave had a value of 3,300 and the
maximum local Mach number M_δ was 1.27.

At a free-stream Mach number of 0.760, laminar separation appears
to have occurred near 0.50 chord, with subsequent transition to turbulent
flow and reattachment being completed by about 0.65 chord (fig. 3(c)).
The change in momentum thickness (fig. 5(c)) in the region of pressure
rise was as abrupt as at the lower free-stream Mach number of 0.736 and
slightly larger in magnitude. The increase in displacement thickness
was of a much larger magnitude than at the lower Mach number and was
followed by an appreciable decrease in value between 0.60 and 0.65 chord
as a result of change to a completely turbulent profile. Beyond 0.65
chord, the displacement thickness increased gradually again. The shape
parameter H showed a decrease from a value of about 4 ahead of the shock
wave to about 1.6 at the end of the abrupt pressure rise. This drop in
the value of the shape parameter H was the result of transition from
laminar to completely turbulent flow, caused by the large pressure increase
through the shock wave. This transitional phenomenon was present in all
three free-stream Mach number conditions of figure 5. Inasmuch as the
values of displacement thickness, momentum thickness, and shape parameter
ahead of the shock wave are essentially the same for the different Mach
numbers shown in figure 5, the increase with Mach number in the magnitude
of the variation of these values through the shock wave is primarily the
result of increasing severity of the shock. The boundary-layer Reynolds
number ahead of the shock wave at a free-stream Mach number of 0.760 was
about 3,300 and the maximum local Mach number M_δ was 1.35.

The laminar-boundary-layer Reynolds numbers quoted previously for
all three of the free-stream Mach numbers appear to be higher than any
values published. However, in comparing these values with those of other

investigations at different Mach numbers, for the purpose of indicating the magnitude of transition Reynolds numbers, cognizance should be taken of the fact that the boundary-layer Reynolds numbers as used throughout this paper are based on viscosity and density at the outer edge of the boundary layer. If the Reynolds number were based on viscosity and density near the surface, the values would be about 2,000 for all three of the free-stream Mach numbers. For the investigation of reference 5, where the flow was essentially incompressible and there was practically no variation of viscosity and density throughout the boundary layer, the boundary-layer Reynolds number at transition was about 2,600.

Turbulent Flow Ahead of the Shock Wave

At a free-stream Mach number of 0.710, boundary-layer profiles (fig. 4(a)) were available only downstream of the shock wave. For these downstream stations the chordwise variation of the boundary-layer parameters θ, δ^*, and H was gradual (fig. 6(a)).

At a free-stream Mach number of 0.734, with a boundary-layer Reynolds number R_θ of 9,800 ahead of the shock wave and a maximum local Mach number of 1.26, the momentum thickness θ and the displacement thickness δ^* increased abruptly in a region of the pressure rise. The shape parameter increased slightly (2.0 to 2.3) in the same region.

At a free-stream Mach number of 0.759 with R_θ of 11,800 ahead of the shock wave and a maximum local Mach number of 1.33, the changes in θ, and particularly in δ^*, were considerably larger than at the lower Mach numbers. The shape parameter increased from 2.0 to 3.1 between 0.55 and 0.575 chord. The boundary-layer profiles of figure 4(c) indicate that local separation was imminent or may have occurred between 0.55 and 0.575 chord. The decrease in shape parameter beyond 0.575 chord indicated an improving flow condition with regard to separation. An analysis based on the method of reference 6, for the conditions under which this result was obtained, indicates that a decreasing value of the shape parameter immediately downstream of the shock wave would be expected. Inasmuch as the values of displacement thickness, momentum thickness, and shape parameter ahead of the shock wave are essentially the same for the different Mach numbers shown in figure 6, the increase with Mach number in the magnitude of the variation of these values through the shock wave is primarily the result of increasing severity of the shock wave.

Comparison at Full Scale of Laminar and

Turbulent Boundary Layers

Comparison of the results obtained with laminar and turbulent boundary layers ahead of shock waves indicates that the increase in momentum thickness and displacement thickness through the shock waves was significantly less when there was a laminar layer ahead of the shock wave. With turbulent flow ahead of the shock wave, the shape parameter increased abruptly through the shock wave; the higher the Mach number, the greater the increase. With laminar flow ahead of the shock wave, the value of the shape parameter decreased considerably. Downstream of the shock wave, the boundary layer was more stable with respect to separation when the flow ahead of the shock wave was laminar. At 0.65 chord, for example, the shape parameter had a value of 1.6 at Mach numbers of 0.736 and 0.760 with laminar flow ahead of the shock wave and values of 2.2 and 2.9 at free-stream Mach numbers of 0.734 and 0.759, respectively, with turbulent flow ahead of the shock wave. In general, then, the laminar boundary layer ahead of the shock wave appeared to have favorable effects on the boundary-layer characteristics a short distance behind the shock wave where both the momentum thickness and the shape parameter were about 50 percent lower than for the turbulent-flow condition.

Effect of Reynolds Numbers on Boundary-Layer

Profiles With Shock Waves

Comparison of the present full-scale results with those of reference 1 obtained at low Reynolds numbers (approximately 1/10-scale, fig. 8) and at about the same maximum local Mach number indicates that the changes in boundary-layer characteristics θ/l, $\delta*/l$, and H through shock waves were of about the same magnitude when the flow ahead of the shock waves was turbulent. However, when the flow ahead of the shock waves was laminar, the changes in θ/l and $\delta*/l$ were about 10 times greater at the low Reynolds numbers (approximately 1/23-scale, fig. 7). The shape parameter some distance downstream of the shock waves approached the same value (1.6) for both investigations. The comparison of the results at high and low Reynolds numbers indicates that, although the laminar flow ahead of a shock wave at low Reynolds numbers would adversely affect the aerodynamic characteristics of an airfoil, at full-scale Reynolds numbers laminar flow ahead of the shock wave would be beneficial, at least with respect to boundary-layer characteristics downstream of the shock wave.

SUMMARY OF RESULTS

A flight investigation was made at free-stream Mach numbers up to 0.76 and Reynolds numbers up to 26×10^6 to determine the effect of shock waves on boundary-layer behavior. The results indicate that, in the region of the pressure rise associated with a shock wave, the rapid increase in momentum thickness and displacement thickness was significantly less when the boundary layer ahead (upstream) of the shock wave was laminar than when it was turbulent. With laminar flow ahead of the shock wave, transition from laminar to turbulent flow was caused by the abrupt pressure rise of the shock wave, and was accompanied by a large decrease in the value of the boundary-layer shape parameter H through the shock wave. The beneficial effect of having laminar flow ahead of the shock wave was indicated by the appreciably lower values of both the momentum thickness and the shape parameter a short distance downstream of the shock wave.

Comparison of the present results with results of other investigations at low Reynolds numbers (up to 1/10-scale) indicates that with turbulent flow ahead of the shock wave the changes in the boundary-layer characteristics through the shock wave were not much different for the full-scale than for the 1/10-scale data. With laminar flow ahead of the shock wave, the changes in momentum thickness and displacement thickness (expressed as a fraction of the characteristic length) were about 10 times as great for the 1/23-scale data as for the full-scale data.

Langley Aeronautical Laboratory,
    National Advisory Committee for Aeronautics,
   Langley Field, Va., September 11, 1953.

REFERENCES

1. Ackeret, J., Feldmann, F., and Rott, N.: Investigations of Compression Shocks and Boundary Layers in Gases Moving at High Speed. NACA TM 1113, 1947.

2. Harrin, Eziaslav N.: A Flight Investigation of the Effect of Shape and Thickness of the Boundary Layer on the Pressure Distribution in the Presence of Shock. NACA TN 2765, 1952.

3. Davies, F. V.: Some Effects of Pitot Size on the Measurement of Boundary Layers in Supersonic Flow. Tech. Note No. Aero. 2179, British R.A.E., Aug. 1952.

4. Donaldson, Coleman duP., and Lange, Roy H.: Study of the Pressure Rise Across Shock Waves Required to Separate Laminar and Turbulent Boundary Layers. NACA TN 2770, 1952.

5. Wetmore, J. W., Zalovcik, J. A., and Platt, Robert C.: A Flight Investigation of the Boundary-Layer Characteristics and Profile Drag of the NACA 35-215 Laminar-Flow Airfoil at High Reynolds Numbers. NACA WR L-532, 1941. (Formerly NACA MR, May 5, 1941.)

6. Von Doenhoff, Albert E., and Tetervin, Neal: Determination of General Relations for the Behavior of Turbulent Boundary Layers. NACA Rep. 772, 1943. (Supersedes NACA ACR 3G13.)
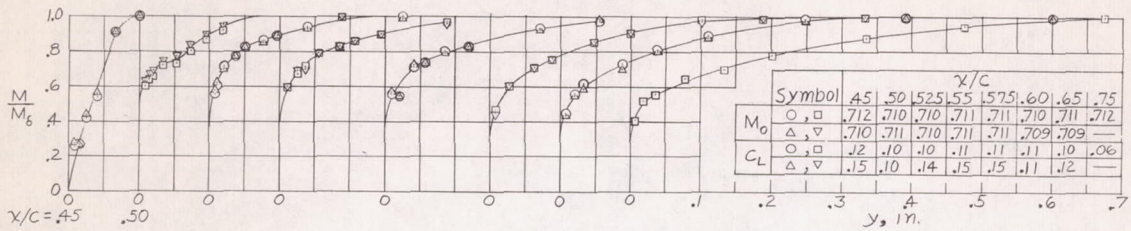
L-47817

Figure 1.- Airplane with airfoils installed on left and right wings
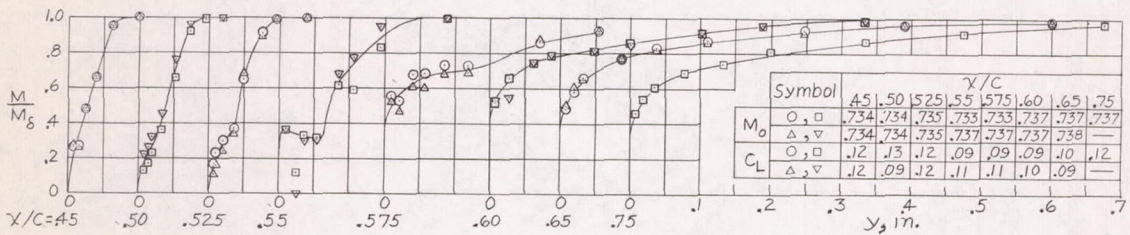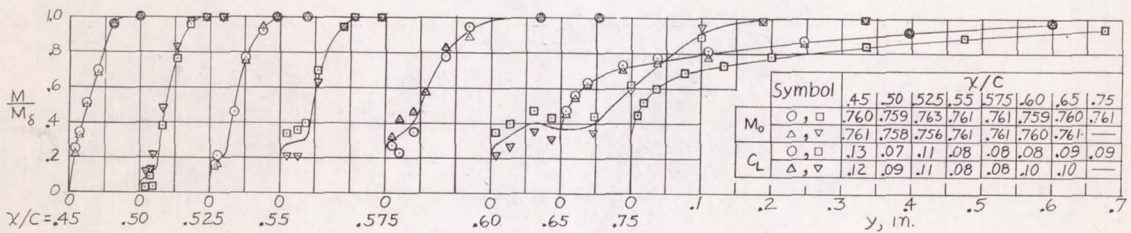(prior to covering test-airfoil surfaces with aluminum sheets).
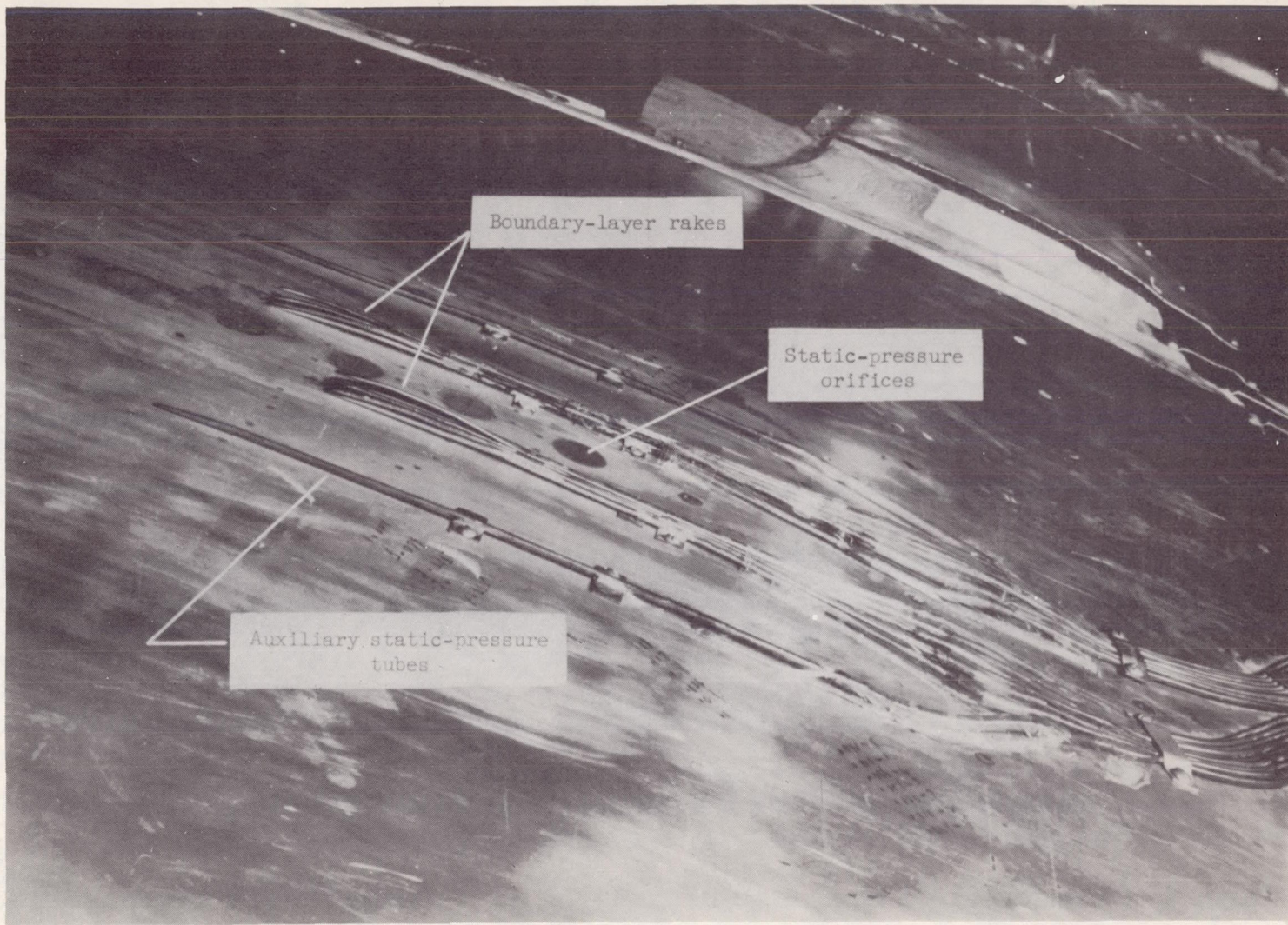
L-64246.1

Figure 2.- Typical arrangement of boundary-layer rakes. Auxiliary static-pressure tubes and surface orifices are also shown.

Symbol	x/c							
	.45	.50	.525	.55	.575	.60	.65	.75
M_0 ○,□	.712	.710	.710	.711	.711	.710	.711	.712
△,▽	.710	.711	.710	.711	.711	.709	.709	—
C_L ○,□	.12	.10	.10	.11	.11	.11	.10	.06
△,▽	.15	.10	.14	.15	.15	.11	.12	—

(a) $M_0 = 0.710 \pm 0.002$; $C_L = 0.10 \pm 0.05$; $R_c = (19.0 \pm 1.8) \times 10^6$.

Symbol	x/c							
	.45	.50	.525	.55	.575	.60	.65	.75
M_0 ○,□	.734	.734	.735	.733	.733	.737	.737	.737
△,▽	.734	.734	.735	.737	.737	.737	.738	—
C_L ○,□	.12	.13	.12	.09	.09	.09	.10	.12
△,▽	.12	.09	.12	.11	.11	.10	.09	—

(b) $M_0 = 0.736 \pm 0.002$; $C_L = 0.11 \pm 0.02$; $R_c = (20.8 \pm 2.5) \times 10^6$.

Symbol	x/c							
	.45	.50	.525	.55	.575	.60	.65	.75
M_0 ○,□	.760	.759	.763	.761	.761	.759	.760	.761
△,▽	.761	.758	.756	.761	.761	.760	.761	—
C_L ○,□	.13	.07	.11	.08	.08	.08	.09	.09
△,▽	.12	.09	.11	.08	.08	.10	.10	—

(c) $M_0 = 0.760 \pm 0.003$; $C_L = 0.11 \pm 0.02$; $R_c = (23.3 \pm 2.5) \times 10^6$.

Figure 3.- Distribution of Mach number through the boundary layer at
various chordwise positions for several values of free-stream Mach
number, as obtained in flight with laminar flow ahead of the shock
wave.
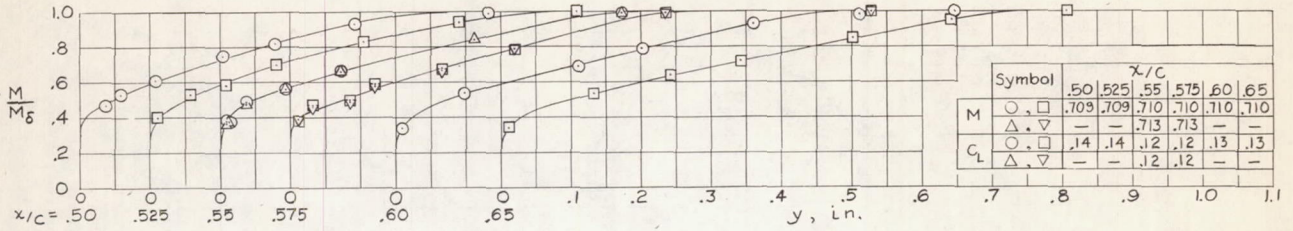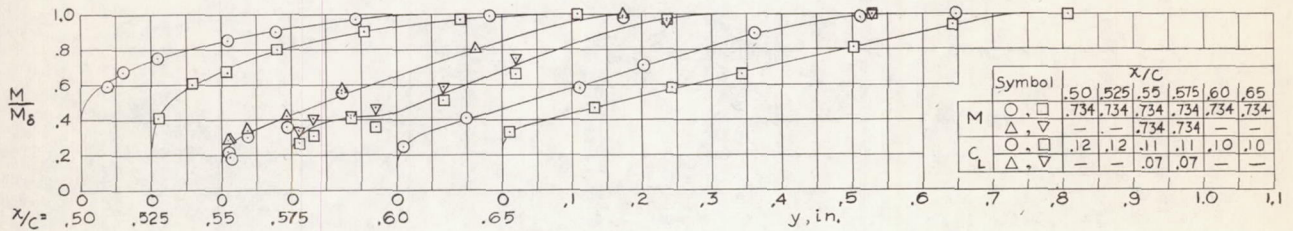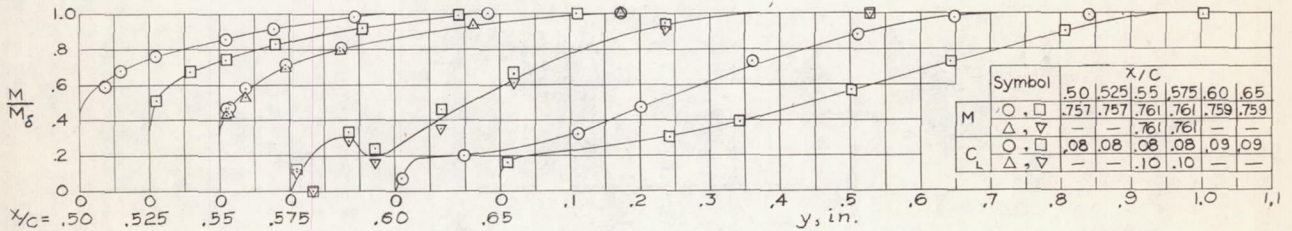
(a) $M_O = 0.710 \pm 0.002$; $C_L = 0.13 \pm 0.01$; $R_c = (16.9 \pm 0.4) \times 10^6$.
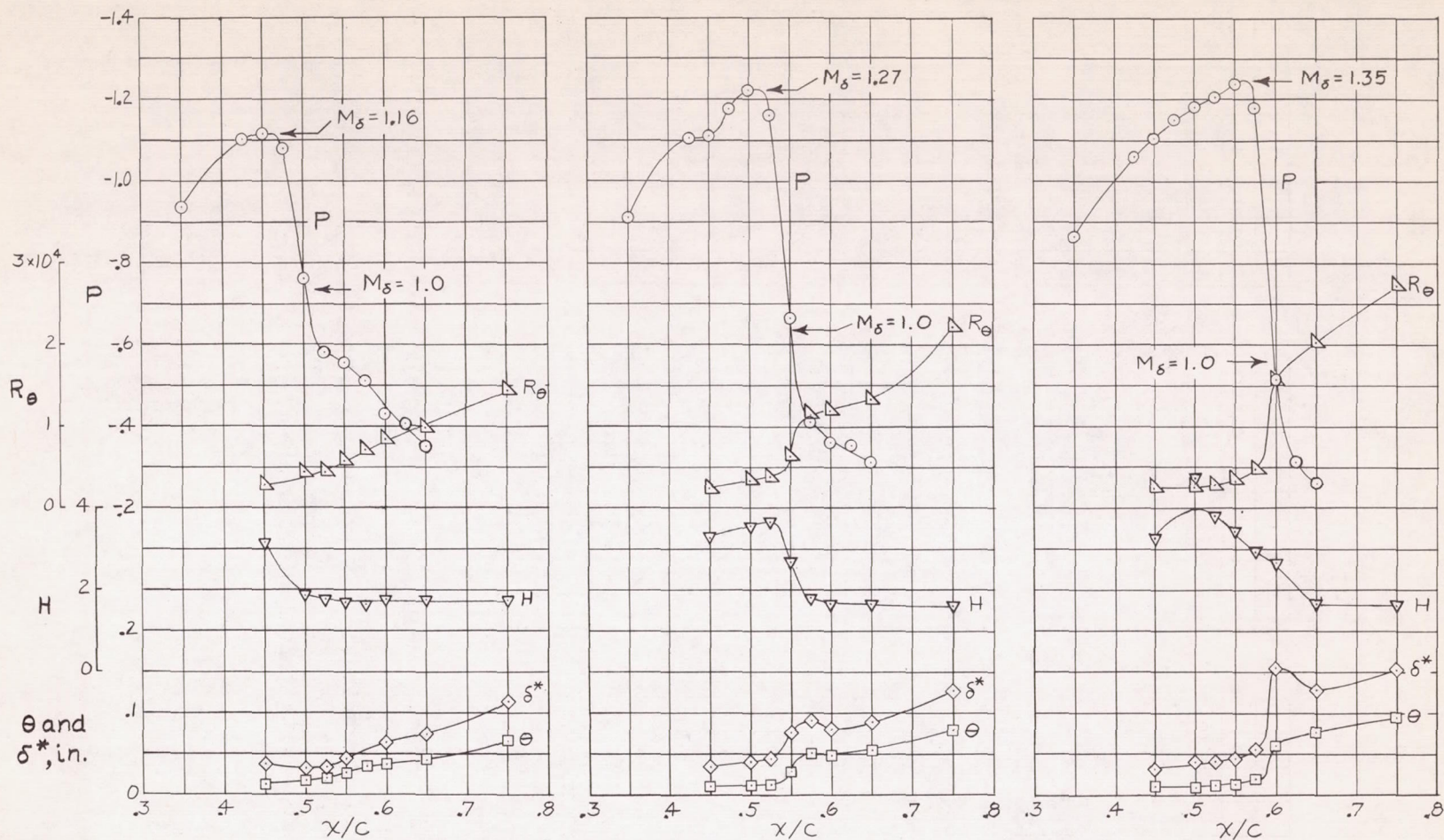

(b) $M_O = 0.734$; $C_L = 0.10 \pm 0.03$; $R_c = (17.9 \pm 0.4) \times 10^6$.

(c) $M_O = 0.759 \pm 0.002$; $C_L = 0.09 \pm 0.01$; $R_c = (19.6 \pm 0.4) \times 10^6$.

Figure 4.- Distribution of Mach number through the boundary layer at
various chordwise positions for several values of free-stream Mach
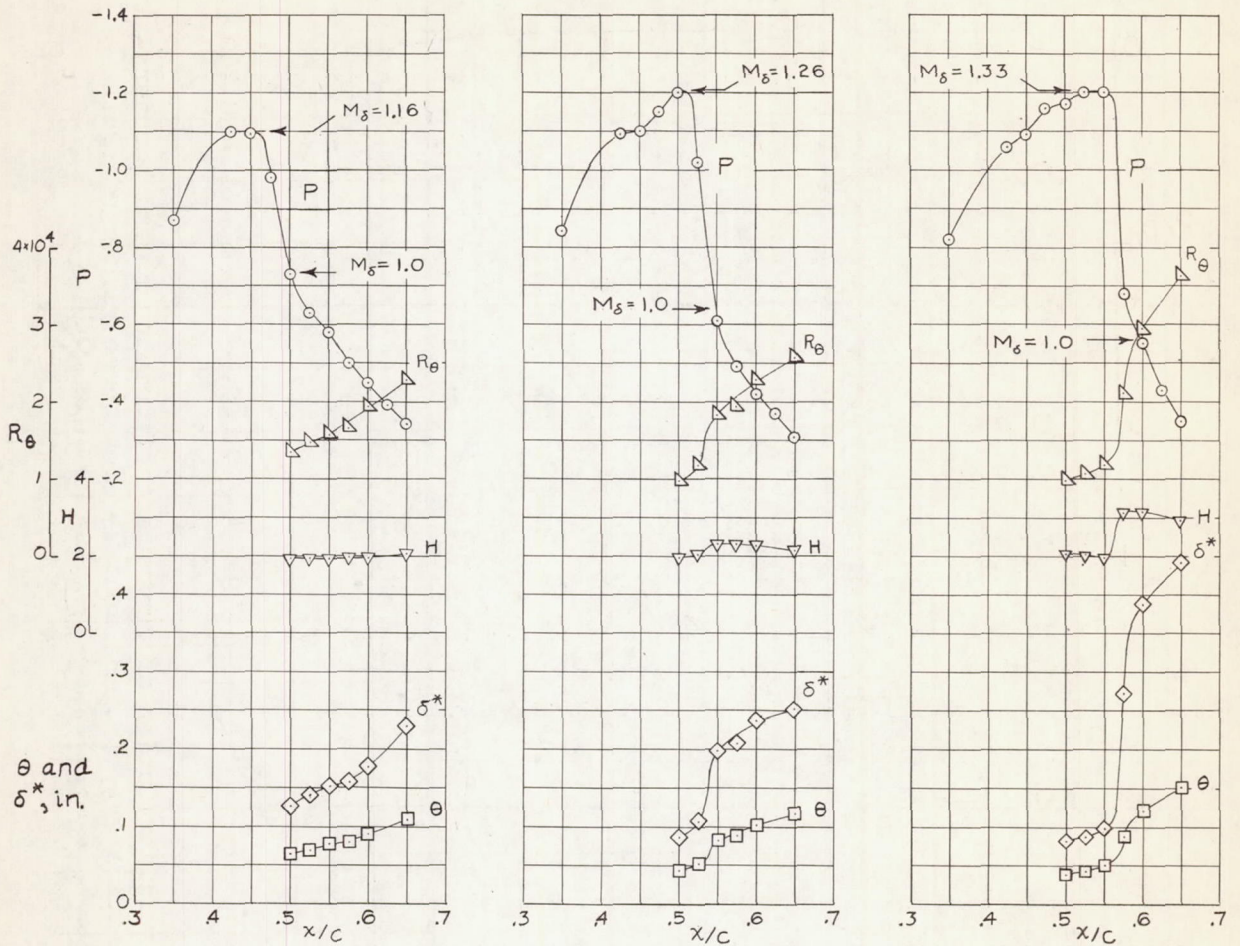number, as obtained in flight with turbulent flow ahead of the
shock wave.

(a) $M_O = 0.710 \pm 0.002$.   (b) $M_O = 0.736 \pm 0.002$.   (c) $M_O = 0.760 \pm 0.003$.

Figure 5.- Chordwise distribution of pressure coefficient P and boundary-
layer characteristics θ, δ^*, H, and R_θ for three values of free-
stream Mach number with laminar flow ahead of the shock wave.

(a) $M_O = 0.710 \pm 0.002$.   (b) $M_O = 0.734 \pm 0$.   (c) $M_O = 0.759 \pm 0.002$.

Figure 6.- Chordwise distribution of pressure coefficient P and boundary-
    layer characteristics θ, δ^*, H, and R_θ for three values of free-
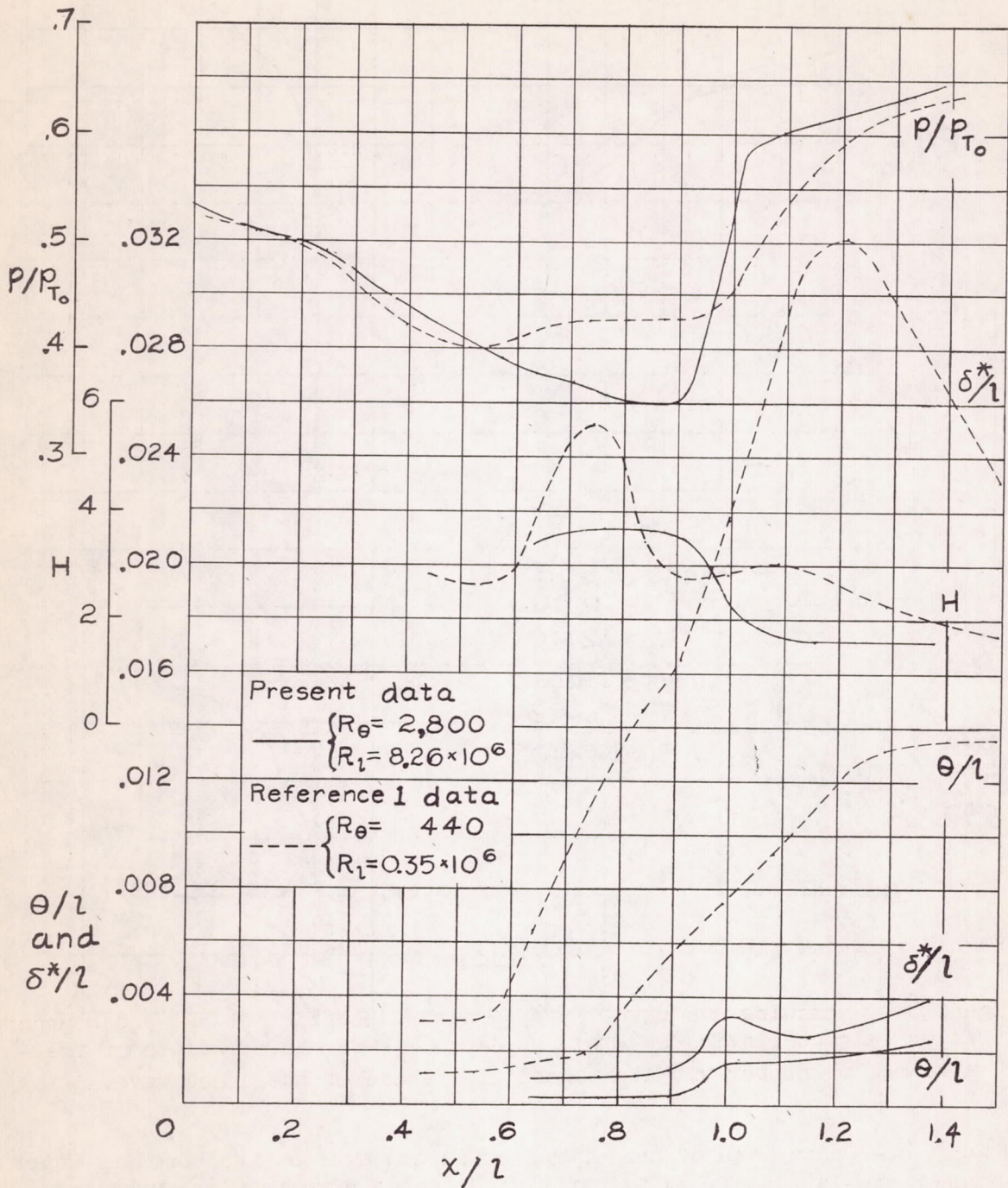   stream Mach number with turbulent flow ahead of the shock wave.

Figure 7.- Comparison of the effect of shock waves on the boundary-layer
characteristics at low and at high Reynolds numbers with laminar
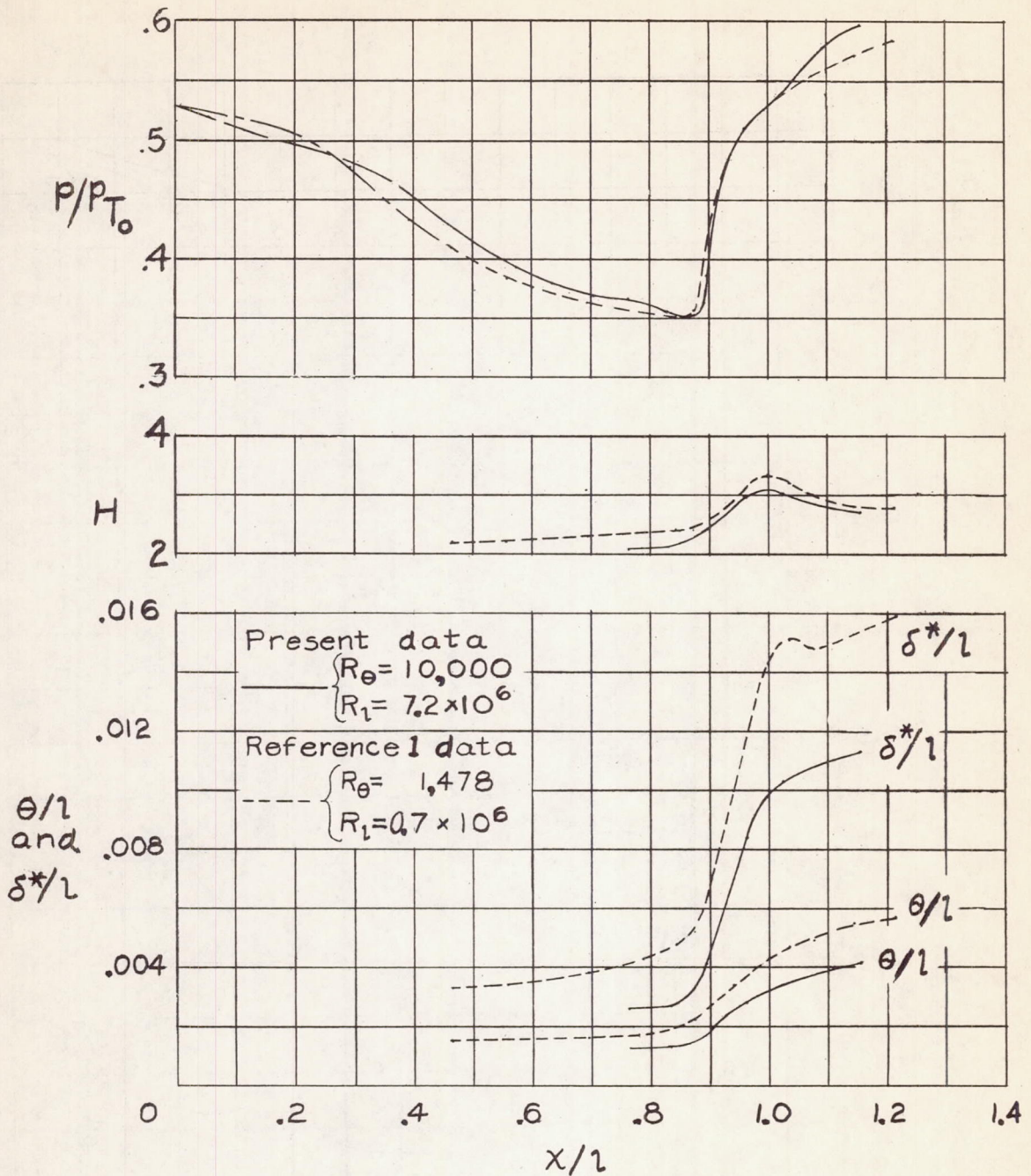boundary layer ahead of the shock wave.

Figure 8.- Comparison of the effect of shock waves on the boundary-layer
   characteristics at low and at high Reynolds numbers with turbulent
   boundary layer ahead of the shock wave.